Article

Bi-directional Free-Space Visible Light Communication (VLC) Supporting Multiple Moveable Clients Using Special Light Diffusing Optical Fiber (LDOF)

Yun-Han Chang [1, 2], Chi-Wai Chow [1, 2*], Yuan-Zeng Lin [1, 2], Yin-He Jian [1, 2], Chih-Chun Wang [1, 2], Yang Liu [3] and Chien-Hung Yeh [4]

[1] Department of Photonics & Graduate Institute of Electro-Optical Engineering, College of Electrical and Computer Engineering, National Yang Ming Chiao Tung University, Hsinchu 30010, Taiwan; yhchang.eo08g@nctu.edu.tw (Y. -H. C.); cwchow@nycu.edu.tw (C. -W. C.); yuanzeng.ee10@nycu.edu.tw (Y. -Z. L.); galaxy8864914@gmail.com (Y. -H. J.); js870102@gmail.com (C. -C. W.)
[2] Department of Photonics & Graduate Institute of Electro-Optical Engineering, College of Electrical and Computer Engineering, National Chiao Tung University, Hsinchu 30010, Taiwan
[3] Philips Electronics Ltd., N.T., Hong Kong; yliu.terse@gmail.com (Y. L.)
[4] Department of Photonics, Feng Chia University, Taichung 40724, Taiwan; yehch@fcu.edu.tw (C. -H. Y.)
* Correspondence: cwchow@nycu.edu.tw

Abstract: Visible light communication (VLC) can offer the advantages of license and electromagnetic interference (EMI) free wireless transmission. As optical signal does not interference with the radio-frequency (RF) signal, VLC can be used to augment RF wireless communication to provide extra communication capacity while without degrading the performance of both signals. In order to achieve high performance VLC transmission, optical alignment between the optical transmit (Tx) and receiver (Rx) is very critical to enhance the received signal-to-noise ratio (SNR). Optical beam-steering at the Tx can be utilized to ensure narrow optical beam can reach the Rx; however, complicated and active tracking are required. Lenses or compound parabolic concentrators (CPCs) can be install in front of the Rx for focusing to enhance the SNR. However, these will limit the Rx field-of-view (FOV) and making the VLC transmission more subjected to misalignment issue. Hence, many creative optical antennas have been proposed and demonstrated using special optical materials as well as special Rx to enhance the FOV of VLC systems. However, they have their limitations, such as data rates and FOVs. In this work, we put forward and demonstrate a bi-direction free-space VLC system supporting multiple moveable Rxs using a light-diffusing optical fiber (LDOF). The downlink (DL) signal is launched from an head-end or central office (CO) far away to the LDOF at the client side via a free-space transmission. When the DL signal is launched to the LDOF, which acts as an optical antenna to re-transmit the DL signal to different moveable Rxs. The uplink (UL) signal is sent via the LDOF towards the CO. In a proof-of-concept demonstration, the LDOF is 100 cm long and the free space VLC transmission between the CO and the LDOF is 100 cm. 210 Mbit/s DL and 850 Mbit/s UL transmissions, meeting the pre-forward-error-correction bit error rate (pre-FEC BER = 3.8×10^{-3}) threshold are achieved.

Keywords: Visible light communication (VLC); Optical wireless communication (OWC); Light diffusing optical fiber (LDOF); Laser diode (LD); Light-diffusing optical fiber (LDOF)

1. Introduction

Due to the great demands for wireless communication bandwidth for applications, such as Internet-of-Things (IoT), online gaming and conferencing, cloud-based storage and processing, etc, the radio-frequency (RF) spectrum has been exhausted. Utilizing the optical frequency spectrum for the future wireless communication, which is known as optical wireless communication (OWC), could be a promising solution [1-5]. Visible light communication (VLC) [6-15] is one implementation of OWC using the visible light spec-

Preprints (www.preprints.org) | NOT PEER-REVIEWED | Posted: 24 April 2023 doi:10.20944/preprints202304.0860.v1

trum. VLC has been developing rapidly in the past decades to provide both communication and illumination simultaneously since it can integrate with the existing light-emitting-diode (LED) illumination infrastructure. Besides, it can offer the advantages of license-free and electromagnetic interference (EMI)-free wireless transmission. As optical signal does not interference with the RF signal, VLC can be used to augment RF wireless communication to provide extra communication capacity while without degrading the performance of both signals. In the future 6G wireless system, VLC is also considered as one of the promising candidates [16, 17]. In addition, VLC could also provide many value-added functions of lighting, including underwater optical wireless communication (UWOC) [18-21], visible light positioning (VLP) [22-25], and optical camera communication (OCC) [26-29].

In order to achieve high performance VLC transmission, optical alignment between the optical transmit (Tx) and receiver (Rx) is very critical to enhance the received signal-to-noise ratio (SNR). At the Tx side, optical beam-steering can be utilized to ensure narrow optical beam can reach the Rx. Optical beam-steering schemes based on mechanical [30], tunable laser [31], diffractive [32], spatial light modulator (SLM) [33], as well as active optical phased array (OPA) [34] approaches have been proposed and demonstrated. Apart from using optical beam-steering schemes, lenses or compound parabolic concentrators (CPCs) [35] can be install in front of the Rx for focusing to enhance the SNR. However, these will limit the Rx field-of-view (FOV) and making the VLC transmission more subjected to misalignment issue, which is the étendue limit issue.

Many creative optical antennas have been demonstrated using special optical materials as well as special Rx to enhance the FOV of VLC systems. In 2016, Peyronel *et al* proposed and demonstrated a tight array of polystyrene fibers doped with an organic dye (Saint-Gobain BCF-92), forming a rectangular detector with increased detection area [36]. They used optical waveguides doped with wavelength shifting dyes. The incident modulated optical signal was absorbed by the dye molecules independently of incidence angle of the optical signal and subsequently re-emitted at a different wavelength. In 2018, Ishibashi *et al* proposed and demonstrated a free-space optical communication (FSOC) system for industrial vehicles using two types of optical fibers (i.e. light-diffusing fiber and wavelength shifting fiber) providing both downlink (DL) and uplink (UL) transmissions [37]. In 2019, Kang *et al* reported a large-area scintillating-fiber-based Rx using ultraviolet (UV)-to-blue color conversion for underwater wireless optical communication [38]. In this scheme, a large-area and wide FOV Rx was achieved to establish a reliable communication link under a turbulent underwater environment. In 2020, Manousiadis *et al* fabricated a wide FOV and high gain fluorescent optical antenna [39]. The structure consisted of a fluorescent material sandwiched between two glass layers. By using different dyes dispersed in transparent epoxy, wavelength division multiplexing (WDM) operation can be realized. In 2020, Riaz *et al* demonstrated a 240° wide FOV VLC Rx for smart phone using a fluorescent fiber [40]. The fluorescent fiber used had a 3-dB response of 80 MHz. By using decision feedback equalization (DFE) with 40 feed-forward and 20 feed-backwards taps, the intersymbol interference (ISI) of the on-off-keying (OOK) signal was mitigated, achieving 1.1 Gbit/s operation. In 2022, Tsai *et al* proposed and illustrated a 360° wide FOV optical camera communication (OCC) system using a phosphor-coated light diffusing fiber [41]. When blue laser diode (LD) was coupled at one end of the light diffusing fiber, blue light was scattered and emitted at the fiber circumference. The yellow phosphor converted the blue light to yellow light; hence, white light was produced by combining the blue and yellow lights. In this system, rolling shutter camera was used; and the data rate was 3.3 kbit/s. Table 1 summaries the performance comparison of recent VLC systems using advanced optical antennas to enhance the FOV.

Table 1. Performance of VLC systems using advanced optical antennas to enhance the FOV

Preprints (www.preprints.org) | NOT PEER-REVIEWED | Posted: 24 April 2023 doi:10.20944/preprints202304.0860.v1

Year	Optical Antenna	Modulation	Data Rate	Antenna Length	FOV	Feature
2016	Polystyrene fiber array (Saint-Gobain BCF-92)	OFDM	2.1-Gbit/s	3.6 × 35 cm	59.4°	Omni-directional detection potential [36]
2018	Light diffusion fiber + wavelength-shift fiber (BCF-92)	OOK	100-Mbit/s (DL) + 100-Mbit/s (UL)	50 m (DL), 25 m (UL)	360°	For industrial vehicles [37]
2019	Scintillating fiber array (Saint-Gobain BCF-10)	OOK	250-Mbit/s	1.2 × 30 cm	360°	Underwater wireless optical communication [38]
2020	Fluorescent layer sandwiched by 2 glass layers	OOK	12-Mbit/s	-	60°	2-color WDM [39]
2020	Fluorescent fiber (Saint-Gobain BCF-20)	OOK	1.1-Gbit/s	7.57 cm	240°	For smart-phone Rx [40]
2022	Phosphor-coated light diffusion fiber	OOK	3.3 kbit/s	100 cm	360°	OCC [41]
This work	Light diffusion optical fiber (LDOF)	OOK	210-Mbit/s (DL) + 850-Mbit/s (UL)	100 cm (DL and UL)	360°	Bidirectional + FSO capability

From Table 1, we can observe that in order to provide hundreds Megabit/s, wide FOV and large VLC detection area, light diffusing fiber can be a promising candidate by allowing 360° wide FOV VLC detection around the fiber circumference. In this work, we put forward and demonstrate a bi-direction free-space VLC system supporting multiple moveable Rxs using a light-diffusing optical fiber (LDOF). The downlink (DL) signal is red color at wavelength of 633 nm, which is launched from an head-end or central office (CO) far away to the LDOF at the client side via a free-space transmission. When the DL signal is launched to the LDOF, which acts as an optical antenna to re-transmit the DL signal to different moveable Rxs. The uplink (UL) signal is green color at wavelength of 520 nm. It is sent via the LDOF towards the CO. In a proof-of-concept demonstration reported here, the LDOF is 100 cm long and the free space VLC transmission between the CO and the LDOF is 100 cm. 210 Mbit/s DL and 850 Mbit/s UL transmissions, meeting the pre-forward-error-correction bit error rate (pre-FEC BER = 3.8×10^{-3}) threshold are achieved.

This paper is organized as: in Section 1, the motivation of the proposed bi-directional free-space VLC system supporting multiple moveable clients using LDOF is introduced. A performance comparison of different recent VLC systems using advanced optical antennas to enhance the FOV is presented. In Section 2, the design and structure of the LDOF acting as the omni-directional optical antenna is discussed. The system architecture, experiment, results and discussion will be presented in Section 3 and Section 4 respectively. Finally a conclusion will be given in Section 5.

2. Design and Structure of the Light-Diffusing Optical Fiber (LDOF)

Traditional optical fiber is used to deliver optical carrier containing data information from one end to the other end. As shown in Fig. 1(a), as the refractive index of the fiber core is higher than the fiber cladding, light is refracted and restrained in the fiber core due to total internal reflection (TIR). The traditional optical fiber is not typically

Preprints (www.preprints.org) | NOT PEER-REVIEWED | Posted: 24 April 2023 doi:10.20944/preprints202304.0860.v1

considered suitable for use as an extended light source. By introducing nanostructure scattering centers in the fiber core, very efficient light scattering through the circumference sides of the optical fiber can be achieved as shown in Fig. 1(b). The proposed LDOF [42, 43] has a silica glass core and acrylate polymer cladding with diameters of 170 μm and 230 μm respectively as shown in Fig. 1(c). By using lower index acrylate polymer cladding, the numerical aperture (NA) of the LDOF is about 0.46. The uniformity of the extracted light in the circumference can be adjusted by controlling the number of scattering sights in the fiber core. These nanostructure scattering centers range in size from 50-500 nm; hence, they can scatter effectively the transmitting light in the visible wavelengths. The scattering loss is about 5 dB/m, while the bending loss is small with minimum bending radius of 5 mm. Table 2 summaries the characteristics of the LDOF used in the experiment.

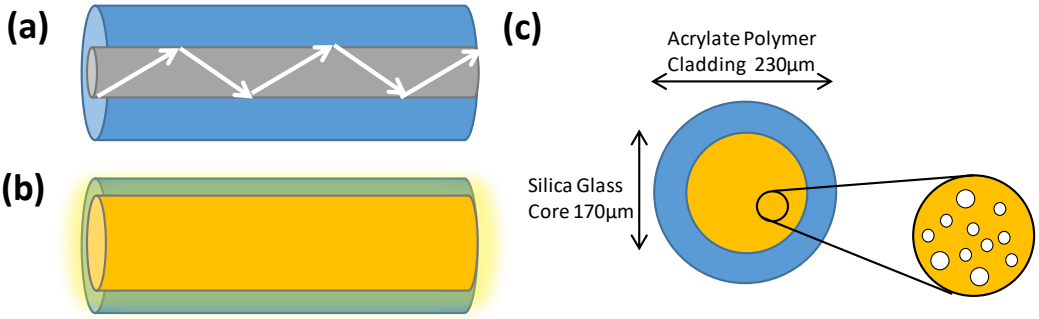

Figure 1. (a) Traditional optical fiber is used to deliver optical carrier containing data information from one end to the other end. (b) LDOF can provide efficient light scattering through the circumference. (c) Cross-section of the LDOF with nanostructure scattering centers in the fiber core for efficient light scattering.

Table 2. Characteristics of the LDOF

Optical or Mechanical Properties	Feature
Diffusion Length	1 m
Numerical Aperture (NA)	> 0.46
FOV Around Fiber Circumference	360°
FOV Along Fiber	120°
Operating Wavelength	420
Core Diameter	170 ± 3 μm
Clading Diameter	230 + 0/ - 10 μm
Proof Test: Tensile Strength	100 kpsi
Operating Temperature	- 20 to + 105 °C

3. Architecture and Experiment of the Bi-directional Free-Space VLC

Fig. 2 shows the proposed system architecture of the bi-directional free-space VLC system, in which the LDOF acts as an optical antenna supporting multiple moveable clients. In order to increase the VLC system flexibility, the LDOF could be installed at a remote location, and the DL data is sent from the head-end office or CO via free-space VLC. The LDOF at the client side acts as an optical antenna to re-transmit the DL signal to different moveable clients. In principle, the system can support a large number of Rxs

Preprints (www.preprints.org) | NOT PEER-REVIEWED | Posted: 24 April 2023 doi:10.20944/preprints202304.0860.v1

simultaneously as long as there are enough space along the LDOF circumference. The UL signal at another wavelength is sent via the LDOF and free-space towards the CO.

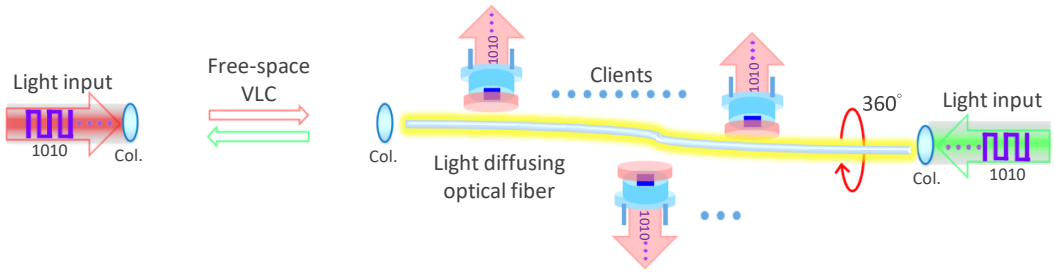

Figure 2. System architecture of the bi-directional free-space VLC system, in which the LDOF acts as an optical antenna supporting multiple moveable clients.

Fig. 3 shows the experimental setup of the free-space VLC system with bi-direction transmissions supporting multiple moveable Rxs. The LDOF is manufactured by Corning®. As discussed in Section 2, nanostructures are added to the inner core to produce light diffusion. The DL and UL Txs are a 633 nm red LD (Thorlabs®, HL63163DG) and a 520 nm green LD (Thorlabs®, PL520) respectively. Two pulse-pattern generators (PPGs) are used to drive the DL and UP LDs at the same time to produce optical on-off-keying (OOK) signals via bias-tees with proper direct-current (DC) biases. At the CO, a dichroic mirror (DM) is employed to separate the red DL and green UL signals. Collimators (Col.) are used to couple optical signals into and out of the LDOF. At the CO, the green UL signal is received by an avalanche photodetector (APD, Thorlabs®, APD210). At the client side, APD (Thorlabs®, APD110A) with a red optical filter (OF) is employ to receive the red DL signal from the LDOF. The client APD can slide along the whole LDOF to receive the DL signal, and the performance will be discussed in next Section. As discussed above, in principle, the system can support a large number of client APDs simultaneously as long as there are enough space along the LDOF circumference. Finally, the received DL and UL OOK eye-diagrams are captured by a digital sampling oscilloscope (DSO) (Agilent®, 86100A); and their BER are measured by a BER tester (Anritsu®, MP1800A).

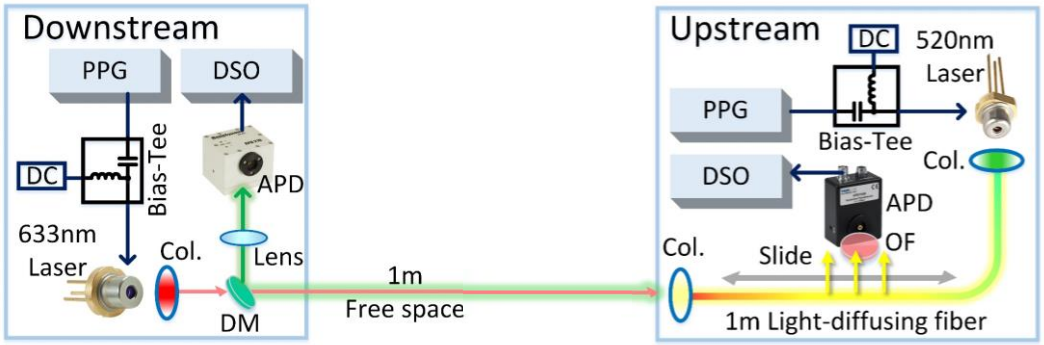

Figure 3. Experimental setup of the free-space VLC system with bi-direction transmissions supporting multiple moveable Rxs. PPG: pulse-pattern generator; APD: avalanche photodetector; DM: dichroic mirror; OF: optical filter; DSO: digital sampling oscilloscope.

4. Results and Discussion

Fig. 4 illustrates the optical powers measured by an optical power meter (Thorlabs®, PM100D) when sliding along the 100-cm LDOF. it can be observed that the light intensity is quite uniform in

Preprints (www.preprints.org) | NOT PEER-REVIEWED | Posted: 24 April 2023 doi:10.20944/preprints202304.0860.v1

the 20 - 80 cm range with an average optical power of 25 μW, illustrating that clients Rx locating at 20 - 80 cm range can receive similar optical signals. It is also worth to point out that as the LDOF is designed to diffuse light 360° around the fiber circumference, the measured optical powers are nearly the same around the LDOF circumference. Fig. 5 illustrates the optical spectra of the DL and UL signals emitted by the 633 nm and the 520 nm LDs measured by a spectrometer (Ocean® Insight USB2000). It can be observed that both the DL and UL signals both have narrow linewidths and high side-mode suppression ratios.

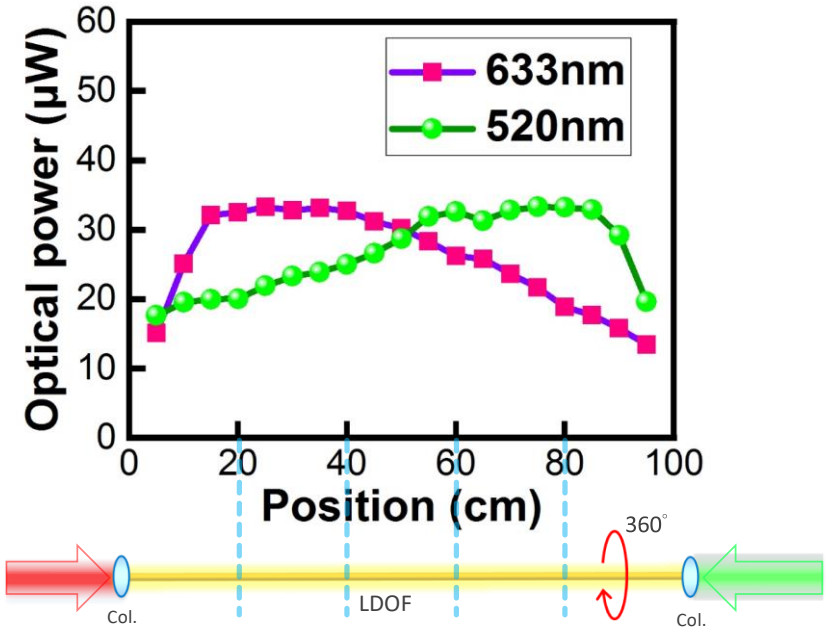

Figure 4. Experimental measured optical powers by a power meter at different positions along the LDOF.

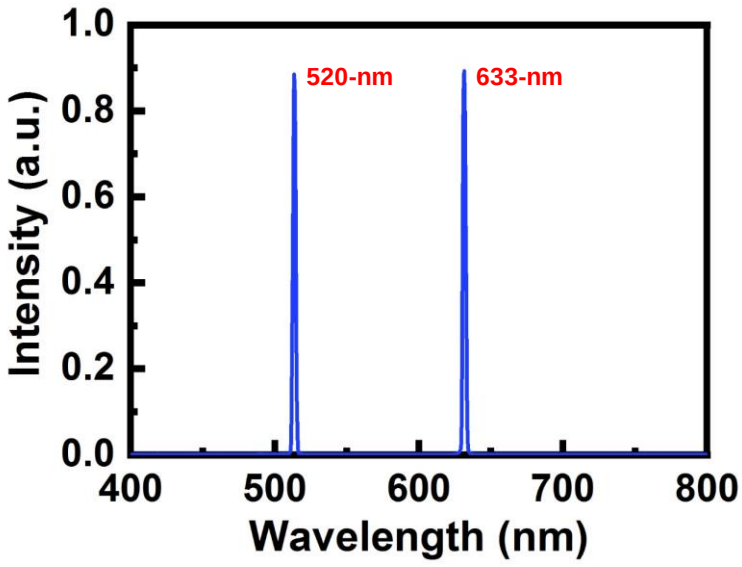

Figure 5. Experimental optical spectrum of both DL and UL signals.

Preprints (www.preprints.org) | NOT PEER-REVIEWED | Posted: 24 April 2023 doi:10.20944/preprints202304.0860.v1

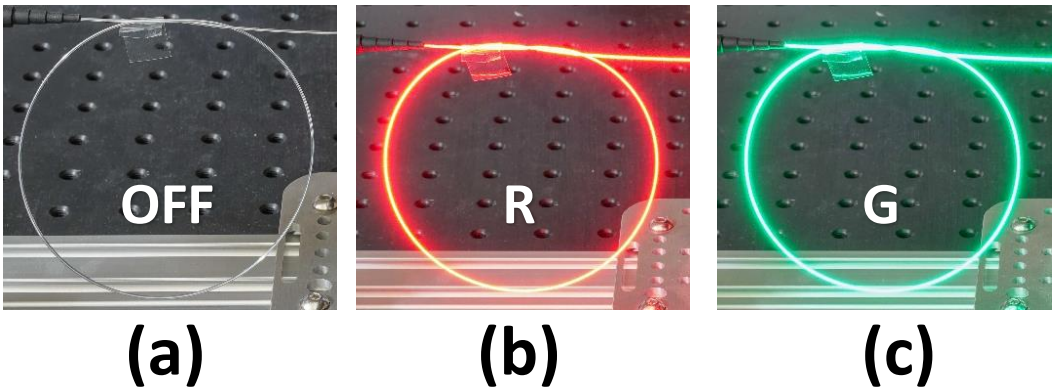

Figure 6. Photographs of the LDOF (a) without, (b) with the red light, and (c) with the green light launchings.

Figs. 6(a)-(c) illustrate the photographs of the LDOF without, with the red light, and with the green light launchings respectively. We can observe uniform light around the fiber circumference in all cases. The optical signal emitted via the LDOF is safe for human eyes. We purposely make turns in the LDOF to illustrate the flexibility of the LDOF as optical omni-directional antenna.

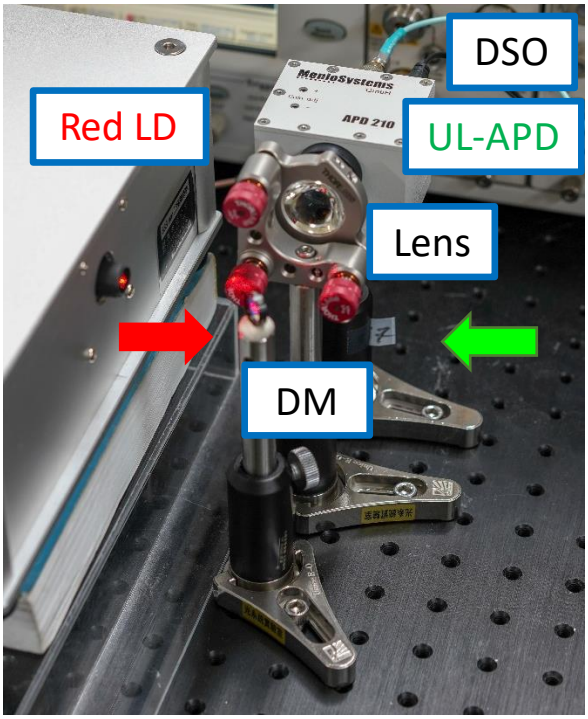

Figure 7. Experimental photographs of the CO. APD: avalanche photodetector; DSO: digital sampling oscilloscope; DM: dichroic mirror.

Fig. 7 illustrates the experimental photographs of the CO, in which a directly modulated red LD is used to provide the DL data, and a APD is used to receive the UL green data. The DM is used to separate the red DL and green UL signals from the wavelength multiplexed signal, and a lens is used to focus the UL signal into the APD. Fig. 8 illustrates the experimental photographs of the client side at different viewing angles. Two collimators at each side of the LDOF are used to couple optical signals into and out of the LDOF. The client APD mounted on a sliding stage can slide along the whole LDOF to receive the DL signal. As discussed above, we purposely make turns in the LDOF to illustrate the flexibility of the optical antenna. Yellow color emitted via the LDOF can be observed when both red and green lights are launched and combined in the LDOF.

Preprints (www.preprints.org) | NOT PEER-REVIEWED | Posted: 24 April 2023 doi:10.20944/preprints202304.0860.v1

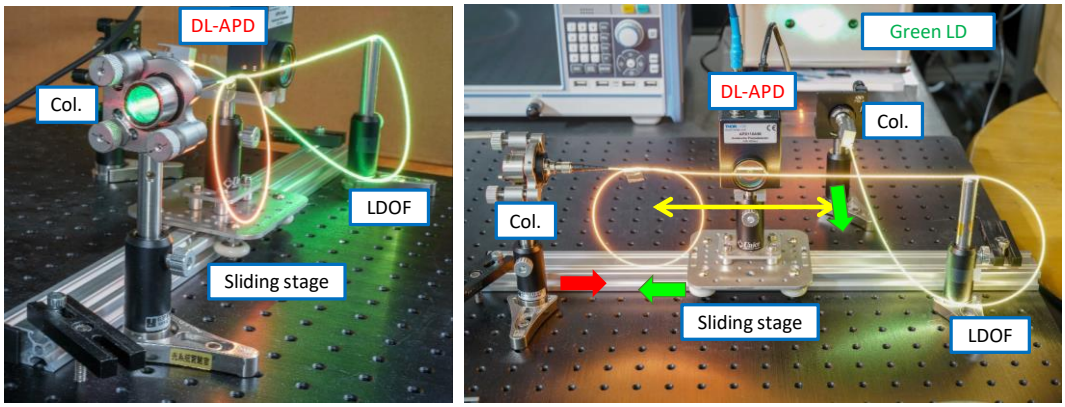

Figure 8. Experimental photographs of the client side at different viewing angles. APD: avalanche photodetector; Col.: collimator; LDOF: light-diffusing optical fiber.

Fig. 9 shows the DL BER measurements via the LDOF from data rates 100 Mbit/s to 220 Mbit/s measured at the client side. From data rate 100 Mbit/s to 190 Mbit/s, it is error-free. BER starts to increase at data rate of 200 Mbit/s, and the BER is 6.50×10^{-7}. BER of 3.69×10^{-4} is measured when the DL data rate is 210 Mbit/s, satisfying the 7% pre-FEC threshold (BER = 3.8×10^{-3}). Fig. 10 shows the corresponding received DL OOK eye-diagrams at different data rates. Clear eye-diagrams can be observed at data rates up to 180 Mbit/s.

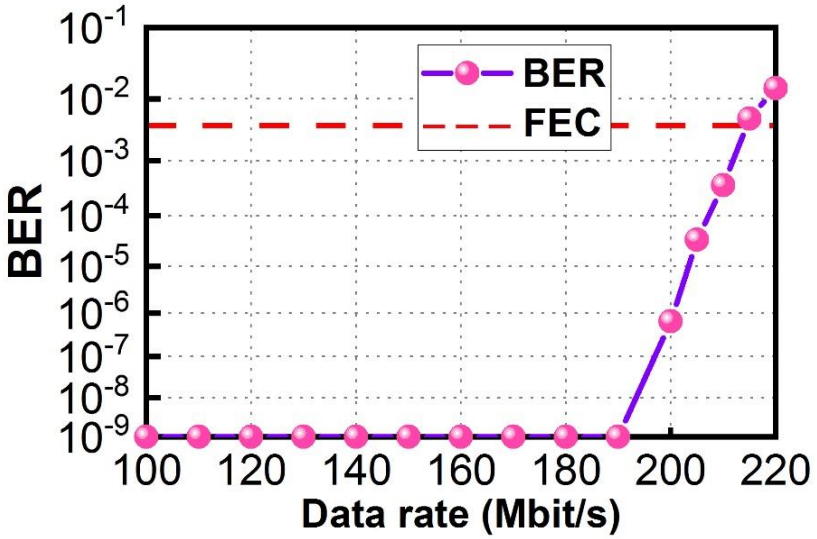

Figure 9. DL BER measurements via the LDOF at the client side.

Preprints (www.preprints.org) | NOT PEER-REVIEWED | Posted: 24 April 2023 doi:10.20944/preprints202304.0860.v1

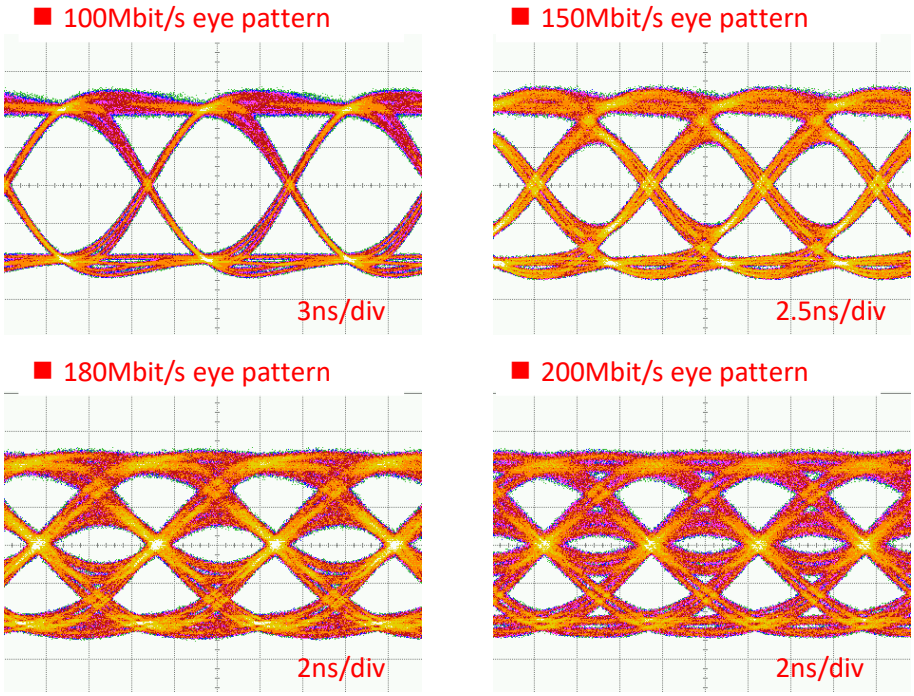

Figure 10. Received DL OOK eye-diagrams.

Fig. 11 shows the UL BER measurement from data rates 100 Mbit/s to 1,000 Mbit/s measured at the CO. From data rate 100 Mbit/s to 600 Mbit/s, it is error-free. BER starts to increase at data rate of 700 Mbit/s, and the BER is 1.14×10^{-6}. BER of 2.15×10^{-3} is measured when the UL data rate is 850 Mbit/s, satisfying the 7% pre-FEC threshold. Fig. 12 shows the corresponding received UL OOK eye-diagrams at different data rates. Clear eye-diagrams can be observed at data rates up to 800 Mbit/s.

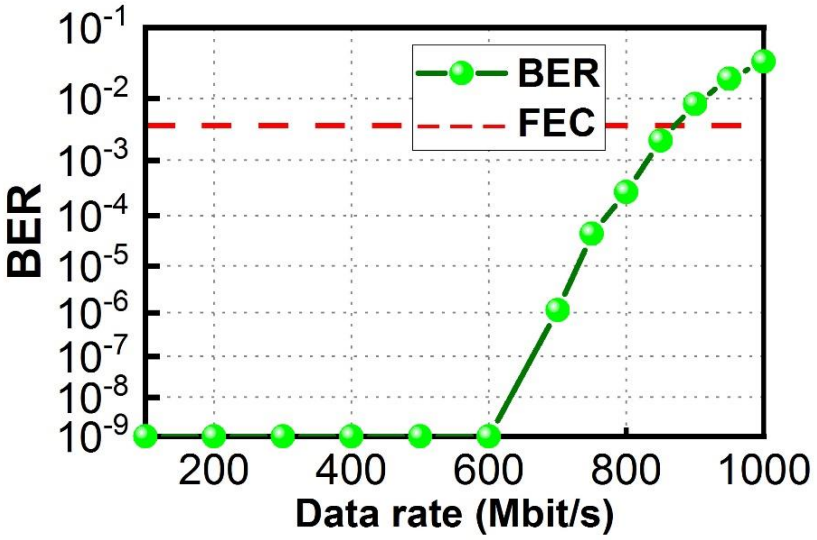

Figure 11. UL BER measurement at the CO.

Fig. 13 shows the DL BER measurement curves at different data rates and at different positions of the 100-cm LDOF optical antenna. We can observe that at date rates of 100, 150 and 190 Mbit/s, error-free detection can be achieved at positions from 10 to 90 cm even the light is not quite uniform along the LDOF as shown in Fig. 4. At data rates of 200 and 210 Mbit/s, we can observe that pre-FEC BER detection (BER = 3.8×10^{-3}) can be achieved for the whole range of LDOF, with the highest BERs are measured at 90 cm locations with BER = 7.60×10^{-5} and 1.30×10^{-3}, respectively. It is also worth to mention that in this proof-of-concept demonstration, a 1-m LDOF is em-

Preprints (www.preprints.org) | NOT PEER-REVIEWED | Posted: 24 April 2023 doi:10.20944/preprints202304.0860.v1

ployed since it is available in the laboratory. 10-m long LDOF is also commercially available, and it can extend the available number of Rxs at the client side. In future work, silicon photomultipliers (SiPM) could also be used to increase the free-space distance between LDOF and the Rx.

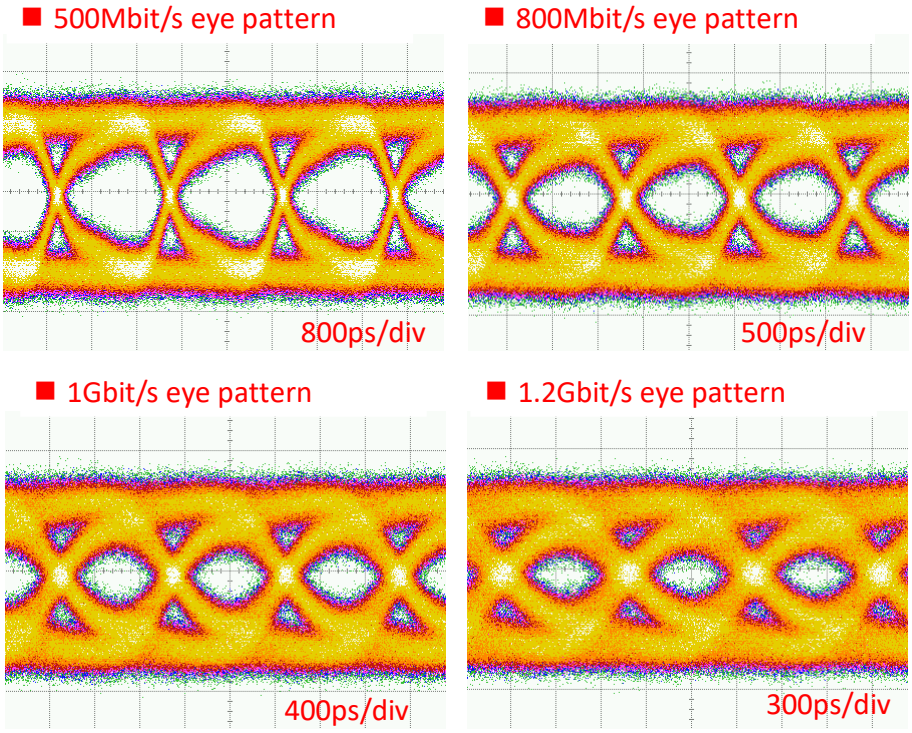

Figure 12. Received DL OOK eye-diagrams.

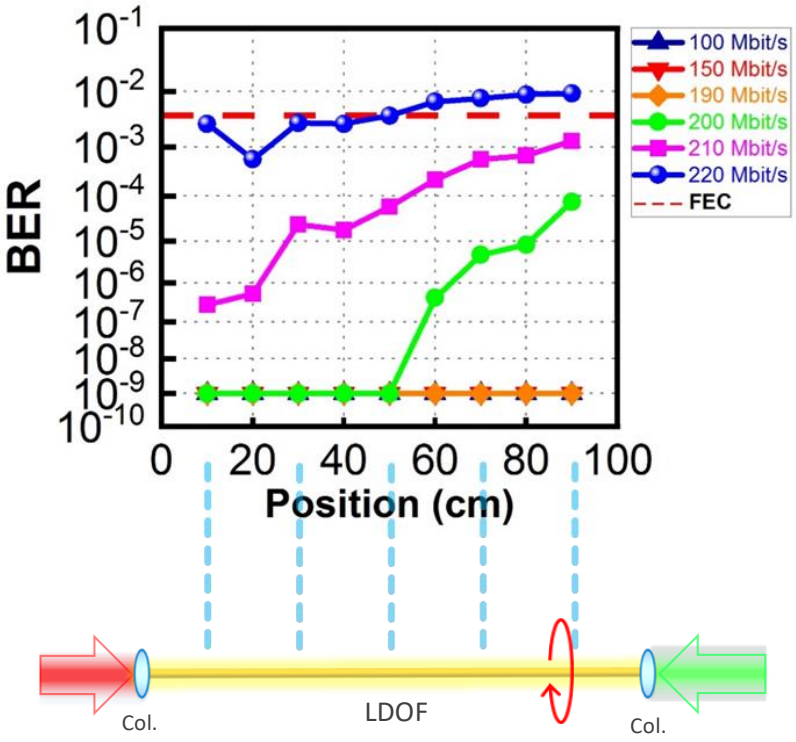

Figure 13. DL BER measurement curves at different data rates and at different position of the 100-cm LDOF optical antenna.

5. Conclusion

In this work, we put forward and demonstrated a bi-direction free-space VLC system supporting multiple moveable Rxs using a LDOF. The proposed LDOF had a silica glass core and acrylate polymer cladding with diameters of 170 μm and 230 μm respectively. The NA of the LDOF was about 0.46. The uniformity of the extracted light in the circumference was adjusted by controlling the number of scattering sights in the fiber core. These nanostructure scattering centers ranged in size from 50-500 nm. The LDOF can provide field-of-views of 360° around the fiber circumference and 120° along the LDOF. In the proposed bi-directional system, the DL signal was launched from a CO away to the LDOF at the client side via a free-space transmission. When the DL signal was at wavelength of 633 nm, and was launched to the LDOF, which acted as an optical antenna to re-transmit the DL signal to different moveable Rxs. The optical signal emitted via the LDOF was safe for human eyes. The UL signal was at wavelength of 520 nm and was sent via the LDOF towards the CO. In a proof-of-concept demonstration, the LDOF was 100 cm long and the free space VLC transmission between the CO and the LDOF was 100 cm. In principle, the system can support a large number of Rxs simultaneously as long as there are enough space along the LDOF circumference. 210 Mbit/s DL and 850 Mbit/s UL transmissions, meeting the pre-forward-error-correction bit error rate (pre-FEC BER = 3.8×10^{-3}) threshold were achieved.

Author Contributions: Data curation, Y. H. Chang, Y. Z. Lin, Y. H. Jian, C. C. Wang; Funding acquisition, C. W. Chow; Investigation, Y. H. Chang, C. W. Chow, Y. Liu, C. H. Yeh; Writing – original draft, Y. H. Chang; Writing – review & editing, C. W. Chow, Y. Liu, and C. H. Yeh.

Funding: This paper was supported by National Science and Technology Council, Taiwan, under Grant NSTC-110-2221-E-A49-057-MY3, NSTC-109-2221-E-009-155-MY3.

Conflicts of Interest: The authors declare no conflict of interest.

References

1. Elgala, H.; Mesleh, R.; Haas, H. Indoor optical wireless communication: potential and state-of-the-art, *IEEE Commun. Mag.*, **2011**, 49, 56–62.
2. Haas, H.; Elmirghani, J.; White I. Optical wireless communication, *Phil. Trans. R. Soc. A.* **2020**, 3782020005120200051.
3. Chow, C. W.; Yeh, C. H.; Liu, Y.; Lai, Y.; Wei, L. Y.; Hsu, C. W.; Chen, G. H.; Liao, X. L.; Lin, K. H. Enabling techniques for optical wireless communication systems, *Proc. OFC 2020*, M2F.1. (Invited).
4. Wang, K.; Song, T.; Wang, Y.; Fang, C.; Nirmalathas, A.; Lim, C.; Wong, E.; Kandeepan S. Evolution of short-range optical wireless communications, *Proc. OFC 2022*, paper Tu3C.4.
5. Wang, K.; Nirmalathas, A.; Lim, C.; Skafidas, E. High-speed indoor optical wireless communication system with single channel imaging receiver, Opt. Express **2012**, 20, 8442-8456.
6. Chow, C. W.; Yeh, C. H.; Liu, Y.; Liu, Y. F. Digital signal processing for light emitting diode based visible light communication, *IEEE Photon. Soc. Newslett.* **2012**, 26, 9-13.
7. Minh, H. L.; O'Brien, D.; Faulkner, Zeng, L.; Lee, K.; Jung, D.; Oh, Y. J.; Won, E. T. 100-Mb/s NRZ visible light communications using a post-equalized white LED, *IEEE Photon. Technol. Lett.*, **2009**, 21, 1063-1065.
8. Vučić, J.; Kottke, C.; Nerreter, S.; Langer, K. D.; Walewski, J. W. 513 Mbit/s visible light communications link based on DMT-modulation of a white LED, J. Lightw. Technol., **2010**, 28, 3512-3518.
9. Chow, C. W.; Yeh, C. H.; Liu, Y. F.; Liu, Y. Improved modulation speed of LED visible light communication system integrated to main electricity network, *Elect. Lett.* **2011**, 47, 867-868.
10. Lu, H. H.; Lin, Y. P.; Wu, P. Y.; Chen, C. Y.; Chen, M. C.; Jhang, T. W. A multiple-input-multiple-output visible light communication system based on VCSELs and spatial light modulators, *Opt. Exp.*, **2014**, 22, 3468-3474.
11. Haas, H. Visible Light Communication, Proc. OFC 2015, paper Tu2G.5.
12. Li, C. Y.; Lu, H. H.; Tsai, W. S.; Feng, C. Y.; Chou, C. R.; Chen, Y. H.; Nainggolan, A. White-lighting and WDM-VLC system using transmission gratings and an engineered diffuser, *Opt. Lett.*, **2020**, 45, 6206–6209.
13. Wu, T. C.; Chi, Y. C.; Wang, H. Y.; Tsai, C. T.; Huang, Y. F.; Lin, G. R. Tricolor R/G/B laser diode based eye-safe white lighting communication beyond 8 Gbit/s, *Sci. Rep.*, **2017**, 7, 11.
14. Tsai, C. T.; Cheng, C. H.; Kuo, H. C.; Lin, G. R. Toward high-speed visible laser lighting based optical wireless communications," *Progress in Quant. Electron.*, **2019**, 67, 100225.
15. Yu, T.-C.; Huang, W.-T.; Lee, W.-B.; Chow, C.-W.; Chang, S.-W.; Kuo, H.-C. Visible Light Communication System Technology Review: Devices, Architectures, and Applications. *Crystals* **2021**, 11, 1098.
16. Chi, N.; Zhou, Y.; Wei Y.; Hu, F. Visible light communication in 6G: advances, challenges, and prospects, *IEEE Vehicular Technol. Mag.*, **2020**, 15, 93-102.

17. Niarchou, E.; Boucouvalas, A. C.; Ghassemlooy, Z.; Alves, L. N.; Zvanovec, S. Visible Light Communications for 6G Wireless Networks, Third South American Colloquium on Visible Light Communications (SACVLC), Toledo, Brazil, **2021**, pp. 01-06, doi: 10.1109/SACVLC53127.2021.9652231.
18. Shen, C.; Guo, Y.; Oubei, H. M.; Ng, T. K.; Liu, G.; Park, K. H.; Ho, K. T.; Alouini, M. -S.; Ooi, B. S. 20-meter underwater wireless optical communication link with 1.5 Gbps data rate, *Opt. Exp.*, **2016**, 24, 25502-25509.
19. Shen, C.; Alkhazragi, O.; Sun, X.; Guo, Y.; Ng, T. K.; Ooi, B. S. Laser-based visible light communications and underwater wireless optical communications: a device perspective, *Proc. SPIE, 10939, Novel In-Plane Semiconductor Lasers XVIII*, 2019, 109390E.
20. Li, C. Y.; Lu, H. H.; Huang, Y. C.; Huang, Q. P.; Xie, J. Y.; Tsai, S. E. 50 Gb/s PAM4 underwater wireless optical communication systems across the water–air–water interface [Invited], *Chin. Opt. Lett*. **2019** 17, 100004.
21. Chen, L. K.; Shao, Y.; Di Y. Underwater and Water-Air Optical Wireless Communication, *J. Lightwave Technol*. **2022**, 40, 1440-1452.
22. Cincotta, S.; Neild, A.; He, C.; Armstrong, J. Visible light positioning using an aperture and a quadrant photodiode, *IEEE Globecom Workshops*, 2017
23. Kim, H. S.; Kim, D. R.; Yang, S. H.; Son, Y. H.; Han, S. K. An indoor visible light communication positioning system using a RF carrier allocation technique, *J. Lightw. Technol.*, **2013**, 31, 134-144.
24. Guan, W.; Wu, Y.; Wen, S.; Chen, H.; Yang, C.; Chen, Y.; Zhang, Z. A novel three-dimensional indoor positioning algorithm design based on visible light communication, *Opt. Commun.*, **2017**, 392, 282–293.
25. Hsu, L.-S.; Chow, C.-W.; Liu, Y.; Yeh, C.-H. 3D Visible Light-Based Indoor Positioning System Using Two-Stage Neural Network (TSNN) and Received Intensity Selective Enhancement (RISE) to Alleviate Light Non-Overlap Zones. *Sensors* 2022, 22, 8817. https://doi.org/10.3390/s22228817
26. Danakis, C.; Afgani, M.; Povey, G.; Underwood, I.; Haas, H. Using a CMOS camera sensor for visible light communication. Proc. OWC'12, 1244–1248.
27. Luo, P.; Zhang, M.; Ghassemlooy, Z.; Minh, H. L.; Tsai, H. M.; Tang, X.; Png, L. C.; Han, D. Experimental demonstration of RGB LED-based optical camera communications, *IEEE Photon. J.*, **2015**, 7, 7904212.
28. Cahyadi, W.A.; Chung, Y.H.; Ghassemlooy, Z.; Hassan, N.B. Optical Camera Communications: Principles, Modulations, Potential and Challenges. *Electronics* **2020**, 9, 1339. https://doi.org/10.3390/electronics9091339
29. Chow, C. W.; Liu, Y.; Yeh, C. H.; Chang, Y. H.; Lin, Y. S.; Hsu, K. L.; Liao, X. L.; Lin, K. H. Display Light Panel and Rolling Shutter Image Sensor Based Optical Camera Communication (OCC) Using Frame-Averaging Background Removal and Neural Network, *J. Lightwave Technol*. **2021**, 39, 4360-4366.
30. Singh, R.; Feng, F.; Hong, Y.; Faulkner, G.; Deshmukh, R.; Vercasson, G.; Bouchet, O.; Petropoulos, P.; O'Brien, D. Design and characterisation of terabit/s capable compact localisation and beam-steering terminals for fiber-wireless-fiber links, *J. Lightw. Technol*., **2020**, 38, 6817–6826.
31. Wu, L.; Han, Y.; Li, Z.; Zhang, Y.; Fu, H. Y. 12 Gbit/s indoor optical wireless communication system with ultrafast beam-steering using tunable VCSEL, *Opt. Exp*., **2022**, 30, 15049.
32. Oh, C. W.; Cao, Z.; Tangdiongga, E.; Koonen, T. Free-space transmission with passive 2D beam steering for multi-gigabit-per-second per-beam indoor optical wireless networks, *Opt. Exp*., **2016**, 24, 19211.
33. Cao, Z.; Zhang, X.; Osnabrugge, G.; Li, J.; Vellekoop, I. M.; Koonen A. M. J.; Reconfigurable beam system for non-line-of-sight free-space optical communication. *Light Sci Appl* **2019**, 8, 69. https://doi.org/10.1038/s41377-019-0177-3
34. Chow, C. W.; Chang, Y. C.; Kuo, S. I.; Kuo, P. C.; Wang, J. W.; Jian, Y. H.; Ahmad, Z.; Fu, P. H.; Shi, J. W.; Huang, D. W.; Hung, T. Y.; Lin, Y. Z.; Yeh, C. H.; Liu, Y. Actively controllable beam steering optical wireless communication (OWC) using integrated optical phased array (OPA), *J. Lightwave Technol.*, **2023**, 41, 1122-1128.
35. Mulyawan, R.; Gomez, A.; Chun, H.; Rajbhandari, S.; Manousiadis, P. P.; Vithanage, D. A.; Faulkner, G.; Turnbull, G. A.; Samuel, I. D. W.; Collins, S.; O'Brien, D. A comparative study of optical concentrators for visible light communications," Proc. SPIE 10128, Broadband Access Communication Technologies XI, 101280L; https://doi.org/10.1117/12.2252355
36. Peyronel, T.; Quirk, K. J.; Wang, S. C.; Tiecke, T. G. Luminescent detector for free-space optical communication, *Optica*, **2016**, 3, 787-792.
37. Ishibashi, M.; Takizuka, H.; Haruyama, S.; Free-space optical communication system for industrial vehicles using two types of optical fibers, *IEEE Globecom Workshops* **2018**, pp. 1-5
38. Kang, C. H.; Trichili, A.; Alkhazragi, O.; Zhang, H.; Subedi, R. C.; Guo, Y.; Mitra, S.; Shen, C.; Roqan, I. S.; Ng, T. K.; Alouini, M. S.; Ooi, B. S. Ultraviolet-to-blue color-converting scintillating-fibers photoreceiver for 375-nm laser-based underwater wireless optical communication, *Opt. Exp*., **2019**, 27, 30450-30461.
39. Manousiadis, P. P.; Chun, H.; Rajbhandari, S.; Vithanage, D. A.; Mulyawan, R.; Faulkner, G.; Haas, H.; O'Brien, D. C.; Collins, S.; Turnbull, G. A.; Samuel, I. D. W. Optical antennas for wavelength division multiplexing in visible light communications beyond the Étendue limit, *Adv. Opti. Mat.*, **2020**, 8, 1901139.
40. Riaz, A.; Collins, S. A wide field of view VLC receiver for smartphones, *Proc. ECOC, **2020***, doi: 10.1109/ECOC48923.2020.9333306.
41. Tsai, D. C.; Chang, Y. H.; Chow, C. W.; Liu, Y.; Yeh, C. H.; Peng, C. W.; Hsu, L. S. Optical camera communication (OCC) using a laser-diode coupled optical-diffusing fiber (ODF) and rolling shutter image sensor, *Opt. Exp*., **2022**, 30, 16069-16077.
42. Logunov, S.; Fewkes, E.; Shustack, P.; Wagner, F. Light diffusing optical fiber for Illumination, Proc. Renewable Energy and the Environment, OSA Technical Digest, **2013**, paper DT3E.4.

 doi:10.20944/preprints202304.0860.v1

43. Corning® Fibrance® Light-Diffusing Fiber Specification.
https://www.corning.com/media/worldwide/csm/documents/Corning_Fibrance_Light_Diffusing_Fiber.pdf